Thrombopoietin Receptor Agonist Eltrombopag Prevents Insulin Resistance and Synaptic Pathology via HIF1α/COX2/Sirt1 Signaling Pathway

he yu
  Wenzhou Medical University First Affiliated Hospital: The First Affiliated Hospital of Wenzhou Medical University

xuebao wang
  Wenzhou Medical College First Affiliated Hospital: The First Affiliated Hospital of Wenzhou Medical University

leping liu
  Wenzhou Medical College First Affiliated Hospital: The First Affiliated Hospital of Wenzhou Medical University

baihui chen
  Wenzhou Medical College First Affiliated Hospital: The First Affiliated Hospital of Wenzhou Medical University

shuya feng
  Wenzhou Medical College First Affiliated Hospital: The First Affiliated Hospital of Wenzhou Medical University

xiaoai lu
  Wenzhou Medical University First Affiliated Hospital: The First Affiliated Hospital of Wenzhou Medical University

ruimin you
  Wenzhou Medical University First Affiliated Hospital: The First Affiliated Hospital of Wenzhou Medical University

Saidan Ding (✉ firstdsdan@hotmail.com)
  Wenzhou Medical University First Affiliated Hospital

Research

Abstract

Background: Insulin resistance has been reported to be closely correlated with the pathogenesis of MHE. The mechanism underlying the effects of thrombopoietin receptor agonist eltrombopag (ELT) on synaptic activity and formation involved in MHE pathogenesis remains unclear.

Methods: The effect of ELT on neurodegeneration and insulin resistance was examined in the primary rat neurons and an MHE rat model.

Results: We found that the level of thrombopoietin receptor c-MPL (MPL) expression was decreased in MHE brains, and ELT administration improved insulin resistance, alleviated the destruction of synaptic formation and enhanced learning and memory in the MHE rats, indicating the relationship between dowregulated ELT and insulin resistance. Then in vitro, ELT treatment ameliorated the impairment of glucose uptake, indicating the reduction of insulin resistance. High dose of glucose inhibited insulin-stimulated downregulation of Hypoxia-inducible factor-1α (HIF1α) expression, the inhibition of inflammatory response and upregulation of sirtuin-1 (Sirt1), destruction of synaptic formation and activity, which were all reversed by ELT treatment in insulin resistant neurons.

Conclusions: These results indicate that ELT is a promising potential therapeutic agent for insulin resistance and defect in learning and memory.

Introduction

Thrombopoietin (TPO), a stimulator of megakaryocytic/platelet lineage, acts in the brain as a counterpart of erythropoietin (EPO), a hematopoietic growth factor with neuroprotective properties. TPO and its receptor c-MPL (MPL) are expressed in the neurons of the human central nervous system (CNS) and murine neural cells. TPO is prominent in human cerebrospinal fluid [1]. TPO was found to be neuroprotective in the CNS in hypoxic-ischemic neonatal rat brain models. TPO reduced brain damage and improved sensorimotor functions. In addition, TPO had a stimulating effect on neural cell proliferation and exerted an antiapoptotic effect [2, 3]. TPO improved neurological function and ameliorated brain edema after stroke [4]. In the developing human CNS, the thrombopoietin gene is abundantly expressed. Considering that thrombopoietin contains a neurotrophic sequence, it may well play a role in neuronal cell biology [5]. Prior to the isolation of TPO, its receptor was identified as the cellular proto-oncogene targeted by murine myeloproliferative leukemia virus and was therefore named MPL. Importantly, TPO and its receptor MPL are expressed in the neurons of the human central nervous system (CNS) and murine neural cells [5–8]. TPO is prominent in human cerebrospinal fluid [1].The biological actions of TPO are initiated by specific binding to its receptors (i.e., MPL) that are expressed on the surface of target cells. Signal transduction from activation of the MPL receptor following TPO binding has been demonstrated in many cell types. Minimal hepatic encephalopathy (MHE) is characterized by a mild impairment in cognition and psychomotor skills, which further progress to a gross impairment in orientation and general consciousness [9, 10].Thus, impaired TPO signaling is critical for the

development of cognitive deterioration in the brain, suggesting that TPO replacement therapy might prevent cognitive disturbance in MHE. Eltrombopag (ELT) is an orally active small molecule thrombopoietin receptor agonist [11]. However, the effect of ELT on cognitive function in MHE remain largely unknown.

Hypoxia-inducible factor-1α (HIF1α) is highly expressed in the adipose tissues of obese individuals and decreases after weight loss [12]. It has been reported that adipocyte-specific HIF1α overexpressing mice develop insulin resistance [13]. Deletion of HIF1α in adipocytes protects mice from HFD-induced insulin resistance [14, 15]. HIF1 is a hetero-dimer consisting of the oxygen regulated HIF1α subunit and the constitutively expressed Hypoxia-inducible factor-1β (HIF1β) subunit [16]. HIF1α is a master regulator of hypoxic responses. Under hypoxic environments, HIF1α subunit is translocated from the cytoplasm to the nucleus, where it dimerizes with the HIF1β subunit and activates the transcription of genes that are required for hypoxic biological responses, including neoangiogenesis and adaptive glucose metabolism [17]. We hypothesized that HIF1α was critically involved in the neuronal insulin resistance. It was suggested that poor cognitive performance in MHE individuals was associated with insulin resistance that regulates learning and memory function via an increased HIF1α expression.

In our previous study, we have demonstrated that insulin resistance was presented in MHE and was associated with the pathogenesis of MHE [18]. In the present study, we tested whether insulin resistance was linked to impairment in learning and memory in MHE accompanied by reduced ELT expression, and whether ELT improved cognitive decline and insulin resistance. This study was aimed at establishing the insulin resistance -mediated HIF1α signaling which signaled to the downstream COX2/sirtuin-1(Sirt1) pathway. However, the underlying mechanisms of memory impairment in MHE was complicated, and here we reported that chronic treatment with ELT protected against the deterioration of recognition and spatial memory in the MHE rat model via the amelioration of insulin resistance.

Materials And Methods

MHE models and treatments

A total of 40 Sprague-Dawley rats (experimental animal center of the Chinese Academy of Sciences in Shanghai) weighing 220–250 g were used.

All experiments were carried out in accordance with the guidelines laid down by the Ethics Committee of the First Affiliated Hospital of Wenzhou Medical University regarding the care and use of animals for experimental procedures.
Before experimentation, all animals underwent two behavioral tests: Y-maze (YM) and water-finding task (WFT). Normal values for these behavioral tests were obtained. Rats were then randomly divided into two groups: a control group (n = 20) and a thioacetamide (TAA) treated group (n = 30). Liver cirrhosis was induced by intraperitoneal injection (i.p.) of TAA (200 mg/kg in normal saline, Sigma-Aldrich,Darmstadt, Germany) twice per week for 8 weeks. TAA-treated rats were diagnosed as hepatic encephalopathy (HE) based on the following symptoms: later development of decreased motor activity, lethargy, and eventual

progression to coma. TAA-treated rats with no HE symptoms were subjected again to behavioral tests to confirm whether MHE had developed. If TAA-treated rats met the alternative criteria for MHE as follows, they were included in the MHE group: a) values of YM lower than mean ± 1.96·SD; b) values of WFT higher than mean ± 1.96·SD [19]. For Thrombopoietin receptor agonist eltrombopag (ELT, Selleck Chemicals #S2229) administration, MHE rats were conducted oral administration (0,5,25mg/kg).

YM test

Rats were individually placed at the end of an arm and allowed to explore the maze freely for 8 min. Total arm entries and spontaneous alternation percentage (SA%) were measured. SA% was defined as the ratio of arm choices that differed from the previous two choices ('successful choices') to total choices during the run ('total entry minus two', because those two entries could not be evaluated) [20].

WFT test

A rat was placed at the near-right corner of the apparatus and allowed to explore it freely for 3 min. Rats were omitted from the analysis when they could not find the tube within the 3-min exploration. After the training session, rats were deprived of water for 24 h. In the trial session, rats were again individually placed at the same corner of the apparatus and allowed to find and drink the water in the alcove. The elapsed times until the entry into the alcove (entry latency, EL), until the touching/sniffing/licking of the water tube (contacting latency, CL) and until the initiation of drinking from the water tube (drinking latency, DL) were measured [21].

Primary hippocampal neurons (PHNs) culture and treatments

The hippocampus was dissected from 14 d gestation Sprague-Dawley rat embryos and placed in ice cold Hank's buffered salt solution (HBSS). Tissues were incubated with 0.25% trypsin in HBSS for 5 min in 37°C/5% CO2. Cells were dissociated by trituration through a glass Pasteur pipet and then passed through a 70 μm cell strainer (Falcon 352350,NY USA). Cells were plated at a density of 200,000 cells/well onto poly-D-lysine/laminin-coated 8-well chamber slides in DMEM + 10% HIFBS + 1% glutamine + 1% Pen-Strep and incubated for 2 h. The medium was aspirated after 2 h and then replaced with selection medium (DMEM + 2.75% SATO serum + 1% glutamine + 1% Pen-Strep) as described. Cultures were incubated in the selection medium for 5 days, and the medium was changed daily to remove dead cells.

Then cells were pre-treated with HIF1α antagonist YC-1 (10μM), HIF1α agonist DMOG (0.5 mM), COX2 antagonist Rofecoxib (1 mM), Sirt1 agonist resveratrol (100 μM), or Sirt1 antagonist nicotinamide (NAM, 3mM) alone or after preincubation with three concentrations of ELT (0, 6.25, 12.5 and 25 μM). After the preincubation period, the cells were stimulated with 100 nM insulin in the presence of normal (5.5mM) or high (30mM) concentration of D-glucose for 24 h.

Assessment of insulin resistance

To induce insulin resistance, primary hippocampal neurons (PHNs) were starved in serum-free DMEM medium with 0.5% (w/v) bovine serum albumin (BSA) for 3 h and pre-treated with normal (5.5mM) or high (30mM) concentration of D-glucose in 10% fetal bovine serum (FBS) DMEM. To evaluate insulin resistance, ^{3}H-2-DG radioactivity taken up by the cells was determined by a scintillation counter. high D-glucose –treated cells showed a significantly lower radioactivity than normal D-glucose -treated cells and were considered to be insulin resistant. These insulin-resistant cells were used for the following experiments.

^{3}H-2-DG uptake measurement

This assay was performed using a modified version of a previously described protocol [10]. Briefly, insulin-resistant cells were starved in serum-free, 0.5% (w/v) BSA DMEM for 3 h before treatment. To confirm insulin resistance, 100 nM insulin was added to the medium for 30 min and then the radioactivity of ^{3}H-2-DG taken up by the cells was determined. To investigate the effects of ELT on glucose uptake or insulin-stimulated glucose uptake, various concentrations of ELT were added to the medium alone or followed by 100 nM insulin for 30 min. To determine the involvement of the HIF1α/COX2/Sirt1 pathway, the 10µM YC-1, 0.5mM DMOG, 1mM Rofecoxib, 100µM resveratrol or 3mM NAM was added to the medium 30 min before ELT treatment, respectively. After washing three times with Krebs–Ringer phosphate buffer (KRP, 1.32 mM NaCl, 4.71 mM KCl_2, 47 mM $CaCl_2$, 1.24 mM $MgSO_4$, 2.48 mM Na_3PO_4, and 10 mM HEPES (pH 7.4)), a final concentration of 1 µCi/ml ^{3}H-2-DG was added to the cells. The medium was aspirated 10 min later, and the cells were washed three times with icecold KRP to terminate the reaction. Next, the cells were lysed with 0.1 N NaOH, and the radioactivity taken up by the cells was determined using a scintillation counter (LS 6500, Beckman Instruments, Fullerton, CA, USA). Nonspecific glucose uptake was measured by subtracting values for ^{3}H-2-DG in the presence of 100 nM cytochalasin B.

Detection of fasting glucose and insulin levels

After the behavior tests, the rats fasted for 12 h, 3 ml of blood samples were collected from each rat and centrifuged at 1200×g, 15min to abtain the serum. The fasting blood glucose levels were determined by a glucose-oxidase biochemistry analyzer and fasting insulin levels were measured by homogeneous phase competitive immunoradiometric assay with an immunoreagent kit using a GC-911c immunoradiometric counter (Enterprises Group of USTC, Hefei, China). The homeostasis model of insulin resistance (HOMA-IR) was calculated using the formula: [fasting glucose (mmol/l) × fasting insulin (IU/mL)]/22.5.

Dendritic spine density analysis in primary neurons

Neural dendritic spine analysis was performed by immunocytochemistry with anti-microtubule-associated protein 2B (anti-MAP2B) and anti-vesicular glutamate transporter 1 antibodies. After fixation, neurons were incubated with primary antibodies anti-MAP2B (MAP2B; 1:200; BD Transduction Laboratories, San Jose, CA, USA) and anti-vesicular glutamate transporter 1 (vGlut1; 1:100; Neuromab,

Davis, CA, USA) overnight at 4°C. Cells were then washed with PBS, incubated with secondary antibody conjugated with AlexaFluor conjugates (1:500; Life Technologies, Waltham, MA, USA) for one hour at room temperature, and coverslipped. A Z stack of optical section was visualized on a confocal laser scanning microscope (FV10i-w, Olympus, Tokyo, Japan). At least 10 cultured neurons from 2 batches of cultures per group were used for quantitative analysis.

Functional labeling of presynaptic boutons with FM4-64

FM4-64 staining (Invitrogen,Carlsbad, CA,USA) was performed according to the manufacturer's instructions. Briefly, primary neurons were incubated with 5 mg/mL FM4-64 (Invitrogen⎕Carlsbad, CA,USA) and 50 mM KCl in HBSS for 1 min at 4°C, and washed with HBSS to remove free FM4-64.

Reverse transcription-polymerase chain reaction (RT-PCR) and Quantitative Real-time PCR (qPCR)

Total RNA was isolated using the Qiagen RNeasy kit (Hilden, Germany) according to the manufacturer's protocol. cDNA was created using oligo (dT), dNTP, 0.1 M DTT, Moloney murine leukemia virus reverse transcriptase, RNaseOUT, and 5× FS Buffer (all from Invitrogen,Carlsbad, CA,USA). For RT-PCR, cDNA was amplified with PCR Master Mix (Promega, Madison, WI, USA). Amplified products were electrophoresed on 2% agarose gels, visualized by EtBr staining, and normalized to GAPDH. For qPCR, mRNA expression was measured by quantitative PCR using SYBR Premix ExTaq and an MX3000 instrument. PCR was performed in a reaction that included 5 μl 2× PCR master mix, 0.5 μl forward primer (10 μM), 0.5 μl reverse primer (10 μM), 2 μl cDNA. The qPCR condition was as follows: an initial denaturation step of 10 min at 95°C; 40 cycles of 95°C for 10 s, 60°C for 60 s, and 95°C for 15 s; and a final step of slow heating from 60°C to 99°C. All samples were normalized to GAPDH to calculate relative mRNA concentrations.

The primers (Invitrogen,Carlsbad, CA,USA) for the murine genes were as follows:

TPO,5'GGTGGACTTCCTCCTTCTCC3'(Forward) and 5'TCGCTAGCTGCTCTGATGAA3'(Reverse); MPL,5'CCTACTGCTGCTAAAGTGGCAA3'(Forward) and 5'CAATAGCTTAGTGGTAGGTAGGA3'(Reverse);

HIF1α, 5'CGTTCCTTCGATCAGTTGTC3' (Forward) and 5'TCAGTGGTGGCAGTGGTAGT3' (Reverse);

HDAC2, 5'GAGCTGTGAAGTTAAACCGACA3' (Forward) and

5'ACCGTCATTACACGATCTGTTG3' (Reverse);

NF-⎕B, 5'GGTGCGGCTCATGTTTACAG3' and 5'GATGGCGTCTGATACCACGG3';

Synaptotagmin, 5'CGGCAAACT GACTGTCATTC3' (Forward) and 5'GCCCCAGTGCTGTTGTAACCA3' (Reverse);

neuroligin1, 5'TGCCATCAACAGACATCACTC3' (Forward) and 5'TCTACCGAGAAGGGACTTGG3' (Reverse).

Immunoblotting

Cerebral cortex tissues or PHNs were harvested in a lysis buffer (Sigma-Aldrich,Darmstadt, Germany). Samples (50 μg protein) were separated by SDS-polyacrylamide gel electrophoresis (PAGE) and electroblotted to PVDF membrane, which was blocked by incubation in 5% non-fat dry milk dissolved in tris buffered saline-Tween (TBS-T) (150 mM NaCl, 50 mM Tris, 0.05% Tween 20). Following transfer, proteins were probed using a primary antibody: MPL, TPO, HIF1α, HIF1β, NF-⬚B, Sirt1, synaptotagmin, neuroligin1, GDNF, PDGF and β-actin (Santa Cruz, CA, USA). Then horseradish peroxidase-conjugated anti-rabbit secondary antibody was used to detect the primary antibodies. After extensive washing, protein bands detected by antibodies were visualized by ECL reagent (Pierce, Rockford, IL, USA) after exposure on Kodak BioMax film (Kodak⬚Rochester, NY, USA).

Immunofluorescence staining, immunohistochemistry and cytochemistry

Frozen brain sections or PHNs cultured on glass coverslips were fixed with 4% paraformaldehyde and then treated with 0.1% Triton X-100 at room temperature. Blocking was with PBS containing 5% normal goat serum for 1 h at room temperature. Sections were then incubated overnight at 4°C with the following primary antibodies: HIF1α, COX2, Sirt1, synaptotagmin, neuroligin1, MAP2 (Abcam, Cambridge, MA, USA). Binding of primary antibodies was detected by incubating the sections for 30 min with Alexa Fluor 488 (green)/Alexa Fluor 594 (red) conjugated secondary antibodies (Abcam,Cambridge, MA, USA).

Statistical analysis

All of the data were expressed as mean ± SD. Data comparisons were analyzed using one-way analysis of variance (ANOVA). All of the data were tested in normal distribution and equal variances, when Back-of-the-envelope test was used to verify the normal distribution, and F-test was applied for determining the equality of variances. Dunnett's post hoc multiple comparison test was applied when significant differences were determined by the ANOVA model. Then P values were made for adjustment by Bonferroni correction. The level of significance was determined by $P < 0.05$ or $P < 0.01$. All analyses were performed with SPSS 18.0 (PASW Statistics 18.0).

Results

ELT decreased HIF1α expression in insulin resistant PHNs

We first determined the effect of ELT treatment on high concentration of D-glucose-induced insulin resistance in vitro by evaluating the glucose uptake by PHNs. Under low dose of D-glucose condition, insulin stimulated glucose uptake by PHNs compared to the basal condition (Fig. 1a). However, under high dose of D-glucose circumstance, insulin slightly but significantly triggered glucose uptake as compared with the basal condition; Moreover, insulin failed to stimulate glucose uptake compared to low concentration of D-glucose group (Fig. 1a). ELT treatment strongly triggered insulin-mediated glucose uptake in a dose-dependent manner under high dose of D-glucose state (Fig. 1a). These data indicated that ELT ameliorated insulin resistance.

HIF1α plays an important part in the pathophysiology of systemic insulin resistance [22]. Thus, we detected whether ELT treatment acted on the insulin resistance-induced HIF1α activity. Insulin stimulated a significant decrease over the basal level in the HIF1α in PHNs under low concentration of D-glucose condition (Fig. 1b). However, under high concentration of D-glucose condition, insulin was able to mildly but obviously decrease HIF1α expression (Fig. 1b). ELT treatment caused a dose-dependent decrease in insulin-stimulated HIF1α levels (Fig. 1b). Through IF staining, we also confirmed hat high ELT treatment tesulted in an obviously decreased fluorescence intensity of HIF1α stimulated by insulin in insulin resistant PHNs (Fig. 1c). Through RT-PCR (Fig. 1d) and qPCR (Fig. 1e), we found that under normal dose of D-glucose state, insulin obviously decreased the HIF1α mRNA levels compared to the basal condition, but caused a slight but significant decrement of HIF1α mRNA levels under high dose of D-glucose condition; however, high ELT treatment further induced a significant increment in HIF1α mRNA level.

As expected, high ELT treatment triggered insulin-mediated glucose uptake under high dose of D-glucose condition, treatment of YC-1 stimulated further elevation of glucose uptake, and treatment of DMOG caused blockade of the effect in PHNs (Fig. 1f). For PHNs, in the case of normal concentration of D-glucose, insulin had no effect on the HIF1β level compared to the basal condition. However, under high concentration of D-glucose circumstance, insulin did not alter the HIF1β levels compared to low D-glucose group and ELT treatment also had no effect on the protein level (Fig. 1g). These results indicated that ELT improved insulin resistance via the downregulation of HIF1α.

ELT inhibits inflammatory response via inhibition of HIF1α expression in insulin resistant PHNs

It has been reported that administration of insulin suppressed the expression of cyclooxygenase2 (COX2) and Nuclear NF-kappaB p65 activation[1], indicating the association of insulin resistance with inflammation. Thus, we examined whether ELT has the effect on the insulin resistance-induced inflammation in the downstream of HIF1α signal. By IB analysis of PHNs under high concentration of D-glucose condition, insulin caused mild but marked decrement of NF-⬚B nuclear translocation (Fig. 2a), ELT treatment further caused a significant decrease in NF-⬚B nuclear translocation, which were enhanced by YC-1 and reversed by DMOG (Fig. 2a). Through IF staining, we also confirmed that high ELT treatment induced a significantly decreased fluorescence intensity of COX2, which were reversed by DMOG in insulin resistant PHNs (Fig. 2b). Through RT-PCR, we found that under high concentration of D-glucose condition, insulin caused slightly significant decrease in NF-⬚B mRNA levels, and high ELT caused a marked decrease in NF-⬚B mRNA level in insulin-resistant PC12 cells, which were enhanced by YC-1 addition and reversed by DMOG (Fig. 2c). ELT treatment obviously triggered insulin-mediated glucose uptake in PHNs under high concentration of D-glucose condition, which was amplified by pretreatment of Rofecoxib (Fig. 2d). These results indicated that ELT induced the blockade of inflammation to inhibit insulin resistance.

ELT increased Sirt1 expression by inhibiting HIF1α/COX2 signaling in insulin resistant PHNs

Sirt1 has been demonstrated to improve insulin sensitivity [23]. Moreover, Sirt1 is essential for maintenance of normal synaptic and cognitive functions [24–26]. We then addressed the effect of ELT on the insulin resistance-induced inhibition of Sirt1 expression at the downstream of HIF1α/COX2 signaling. As indicated by Fig. 3a, under high concentration of D-glucose condition, insulin incubation triggered a slightly significant increment of Sirt1 expression in PHNs, and ELT addition caused a remarkably significant increase in Sirt1 levels, which was enhanced by YC-1 or Rofecoxib and reversed by DMOG. We also confirmed by IF staining that high ELT treatment induced a significant increase in the insulin-stimulated Sirt1 fluorescence intensity, which was reversed by DMOG in high glucose-induced insulin resistant PHNs (Fig. 3b). Through q-PCR, we found that under high concentration of D-glucose condition, insulin caused a slight but significant increment of Sirt1 mRNA levels in PHNS. High ELT treatment further significantly increased insulin-stimulated HDAC2 mRNA level, which was enhanced by the administration of YC-1 or rofecoxib and reversed by DMOG (Fig. 3c). Pretreatment of resveratrol caused further elevation of insulin-mediated glucose uptake induced by ELT treatment, and pretreatment of NAM caused blockade of the effect in high glucose-induced insulin resistance in PHNs (Fig. 3d). These results indicated ELT ameliorated insulin resistance via upregulation of Sirt1.

ELT has the effect on insulin-stimulated synaptic formation via HIF1α/COX2/Sirt1 signaling in insulin resistant PHNs

Next, we addressed the mechanism of the effect of ELT on the insulin resistance –induced impairment of synaptic formation. As determined by IB analysis for PHNs under high concentration of D-glucose, insulin treatment caused a slight but significant increment of expressions of synaptotagmin and neuroligin1 (Fig. 4a), and ELT treatment caused vastly significant increases in insulin-mediated synaptotagmin/neuroligin1 levels, which was enhanced by pretreatment of YC-1, Rofecoxib or resveratrol (Fig. 4a). High ELT treatment also induced vastly obvious increases in insulin-stimulated GDNF/PDGF levels, whearas pretreatment of DMOG or NAM reversed the two proteins levels in high glucose-induced insulin resistant PHNs (Fig. 4b). RT-PCR showed that, under high concentration of D-glucose condition, ELT treatment caused the vastly significant increase in insulin-stimulated synaptotagmin mRNA level in PHNs, which was enhanced by pretreatment of YC-1, Rofecoxib or resveratrol (Fig. 4c). We also found that high ELT treatment also caused the exceedingly obvious increase in insulin-stimulated neuroligin1 mRNA level, whearas pretreatment of DMOG or NAM reversed the protein levels in insulin resistant PHNs (Fig. 4d).

Double IF staining with anti-vGluT1 (for staining dendritic spines) and anti-MAP2B (for staining microtubules) antibodies revealed that ELT treatment significantly increased insulin-stimulated vGluT1-positive signals in insulin-resistant PHNS cells, whearas pretreatment of DMOG or NAM reversed this reaction (Fig. 4e and f). Using FM4-64 dye to probe activity-dependent synaptic vesicle recycling revealed that high ELT treatment seriously increased insulin-stimulated synaptic activity in insulin-resistant PHNS cells, which was reversed by DMOG or NAM (Fig. 4g and h). These results suggest that ELT facilitated insulin resistance-impaired synaptic formation.

ELT increased MPL expression in MHE rats

We examined MPL expression in the brain tissues of the MHE rats. RT-PCR and qPCR showed reduced MPL transcription levels in cortex of MHE rats (FigureS1a and b) and decreased TPO mRNA in hippocampus of MHE rats (Figure S1c and d). These results suggest that MPL was negatively associated with pathogenesis of MHE. Then the effect of ELT on the MPL expression was addressed. Based on immunoblotting, the cortex (Fig. 5a) of the MHE rats displayed significant reductions in the MPL level, which were rescued by ELT administration, whereas, the decrease in TPO levels in hippocampus of the MHE rats was also blocked by ELT administration (Fig. 5b).

ELT administration improved memory impairment and insulin resistance in MHE rats

Next, we tested the effect of ELT administration on cognitive decline of MHE rats in vivo. In the YM test, the SA% of MHE rats was obviously lower than that of control rats, and the decrease was reversed by high dose of ELT administration (Figure S2a). In the WFT test, the significant increases in EL, CL, and DL of MHE rats were recovered to the normal level by administration of high dose of ELT (Figure S2b). These results suggest that the ELT improved the cognitive deficit.

Our previous study reported that insulin resistance was involved in memory disorder in MHE [18]. We hypothesized that the downregulation of ELT played roles in insulin resistance in the MHE rats. Therefore, the impact of ELT on the insulin resistance was tested. As seen from Table 1, for plasma in MHE rats, not only was the level of fasting glucose obviously elevated, but the insulin level was also markedly elevated, which were both reversed by high ELT administration; and the evaluation of insulin sensitivity by the HOMA-IR index showed that high ELT administration significantly reduced the HOMA-IR index. These data indicate that the ELT has the ability to ameliorate insulin resistance.

ELT decreased HIF1α expression and increased Sirt1 expression in vivo

Next, we investigated the effect of ELT on the HIF1α and Sirt1 expression in MHE rats. As shown in Fig. 6a, the increased HIF1α level and decreased Sirt1 level were observed in the cortexes of MHE rats, and administration of a high dose of ELT significantly restored the expression of the protein. However, a low dose of ELT had no effect on the protein level in MHE rats. IB analysis showed the increase in HIF1α protein level and decrease in Sirt1 level in the hippocampi of MHE rats, and high ELT reversed the changes of the two proteins (Fig. 6b). Using IF staining demonstrated that the decrease in Sirt1 fluorescence intensity was blocked by high ELT administration in the cortices of MHE rats (Fig. 6c). We also confirmed that high ELT recovered the increased HIF1α fluorescence intensity to the normal level in the hippocampi of MHE rats (Fig. 6d). These results confirm that ELT has the protective effect on the HIF1α/Sirt1 signaling in MHE.

ELT increased synaptic formation in vivo

We then tested the effect of ELT on the synaptogenesis in MHE rats. We also observed the reduction of synaptotagmin/neuroligin1 expression in the cortexes of MHE rats, whereas high ELT administration

inhibited the reduction of the two proteins dose-dependently (Fig. 7a). The hippocampi of MHE rats showed decreased protein levels of GDNF/PDGF, which were also abrogated by high ELT (Fig. 7b). As shown by IF staining, high ELT administration increased neuroligin1 fluorescence intensity in the cortices of MHE rats (Fig. 7c). The strong immunofluorescence of GDNF was induced in the hippocampi of MHE rats after ELT (Fig. 7d). These results suggest that ELT has the ability to improve the deterioration of synaptogenesis in MHE.

Discussion

Thrombopoietin (TPO), a 70-kDa glycoprotein, is the primary regulator of megakaryopoiesis and the primary hematopoietic growth factor responsible for platelet production [27]. TPO shows significant homology with EPO (23%) at the amino-acid level and with neurotrophins (e.g., the highest homology with BDNF, 36%) in the N-terminal region [28]. MPL is predominantly expressed on megakaryocytes, mature platelets, and a subset of CD34⯑ hematopoietic stem cells [29]. Importantly, both Tpo expression and cMpl expression have also been detected in nonhematopoietic tissues, including the brain [5–8]. TPO was found to be neuroprotective in the CNS in hypoxic-ischemic neonatal rat brain models. TPO reduced brain damage and improved sensorimotor functions. In addition, TPO had a stimulating effect on neural cell proliferation and exerted an antiapoptotic effect [2, 3]. TPO improved neurological function and ameliorated brain edema after stroke [4]. In the developing human CNS, the thrombopoietin gene is abundantly expressed. Considering that thrombopoietin contains a neurotrophic sequence, it may well play a role in neuronal cell biology [5]. Little is known about the relationship between MPL and neuron protection, synaptic plasticity, and memory function. We found the downregulation of MPL in MHE rats. We uncovered that ELT administration facilitates upregulation of MPL. Our results indicate that MPL plays an important role in cellular mechanisms underlying synaptic formation in MHE rats. In our previous study, we have demonstrated that insulin resistance was presented in MHE and was associated with the pathogenesis of MHE [18]. Insulin resistance combined with reduction of MPL level contributed to the pathogenesis of MHE. In the current study, the results indicated that the insulin resistance occurred in MHE rat brains and cognition impairment was reversed after ELT administration. Finally, MPL and TPO were recently speculated to contribute to insulin resistance-mediated pathogenesis of MHE.

Hypoxia-inducible factor 1 (HIF-1) is a basic helix-loop-helix-PAS domain transcription factor that is expressed in all metazoan organisms and is composed of HIF-1alpha and HIF-1beta subunits [30]. Under hypoxic conditions, HIF-1 regulates the transcription of hundreds of genes in a cell type-specific manner [30]. Nuclear HIF-1α protein translocation in hypoxia-activated astrocytes may be a potential target for ameliorating cognitive impairment [31]. hippocampal HIF-1α appears to be involved in an upstream mechanism of cognitive impairment [32]. HIF-1α represents a critical transcriptional regulator in regenerating neurons and suggests hypoxia as a tool to stimulate axon regeneration [33]. Astrocyte HIF supports synaptic plasticity and learning upon hypoxia [34].The relationship between brain tissue-specific Hypoxia-inducible factor-1α (HIF-1α) and insulin resistance has been explored [14, 15]. Our results indicate that insulin resistance-induced HIF1α activation plays a key role in cognitive impairment. Insulin resistance could inhibit synaptic formation by altering the HIF1α activity. ELT is able to potently modulate

insulin resistance-mediated HIF1α activity. This study also showed a linear relationship between insulin resistance and ELT reduction, and between ELT expression and cognitive functions. Our present study demonstrated that ELT is involved in regulating glucose uptake and synaptic formation via HIF1α signaling pathway. Our experiments provide evidence that the activation of HIF1α signaling is closely related to insulin resistance-regulated synaptic activity, and this effect was reversed by ELT. In this study, we identified HIF1α as a primary downstream effector of insulin resistance, essential for the signaling of synaptic formation. Our study evaluated the ability of insulin resistance to modulate the activity of HIF1α signaling as this is a potential mechanism for insulin resistance-induced downregulation of synaptic proteins. Thus, HIF1α signaling may represent an important target for insulin resistant signaling, and ELT could modulate insulin resistance by altering HIF1α state.

The neuronal expression of = cyclooxygenases-2 (COX-2) may be involved in important physiology functions like synaptic transmission, neuroplasticity, and neuropeptide release [35]. Activating the NF-kB signaling pathway induced cognitive impairment and neuroinflammation [36].Moreover, increased expressions of inflammatory mediators such as cyclooxygenase2 (COX2), nuclear factor kappa B (NF-kB), tumor necrosis factor (TNF-α), were associated with cognitive impairment [37].Cox2 inhibition prevents cognitive impairment in a mouse model of AD and amyloid beta peptide (Aβ)-induced inhibition of long-term potentiation (LTP) [38].Insulin pretreatment significantly prevented changes in levels of proinflammatory markers, triggered translocation of p65 NF-kB, and over expression of TNF-α, IL-1β, COX-2 [39, 40].HIF-1α activated the TGF-β/Smad and TLR4/MyD88/NF-κB pathways [41]. HIF-1α activates NF-κB, that NF-κB controls HIF-1α transcription and that HIF-1α activation may be concurrent with inhibition of NF-κB. NF-κB is a critical transcriptional activator of HIF-1α and that basal NF-κB activity is required for HIF-1α protein accumulation under hypoxia in cultured cells and in the liver and brain of hypoxic animals [42]. HIF-1αis involved in the regulation of COX-2 expression [43]. IL-1β mediated NFkB-dependent COX-2 expression served as a positive effector for HIF-1αa induction. IL-1β up-regulates functional HIF-1αa protein through a classical inflammatory signaling pathway involving NFkB and COX-2 [44]. We reported that insulin resistance may exert its stimulant effects on COX2 expression and NF-⬚B translocation through the HIF1α pathway. Insulin resistance-stimulated COX2 upregulation appears to be dependent upon the activation of HIF1α. ELT causes a decrease in COX2 expression and NF-⬚B translocation, which are sensitive to insulin, leading to the synaptic formation via HIF1α.

The mammalian Sir2 homologue Sirt1 is a redox-sensitive nicotinamide adenine dinucleotide+ (NAD+)-dependent deacetylase. Sirt1 plays a critical role in metabolism and anti-aging effects [45]. The activation of Sirt1 has been shown to retard the aging process [46], as well as to attenuate neurodegeneration [47]. A wealth of data has shown that Sirt1 plays an important role in insulin resistance and type 2 diabetes [48]. Previously, a reduced hepatic Sirt1 level has been shown to lead to hepatic insulin resistance and type 2 diabetes [49]. Sirt1 depletion in adipocytes inhibits insulin-stimulated glucose uptake [50]. Sirt1 is regarded as a link between metabolism and aging [51]. Sirt1 overexpression or small chemical Sirt1 activators showed beneficial effects of Sirt1 activation on glucose homeostasis and insulin sensitivity [52]. Sirt1 has been demonstrated to promote glucose homeostasis by enhancing beta cell function [53] and to improve insulin sensitivity in skeletal muscles [23]. Sirt1, a nuclear histone deacetylase, could

influence cellular function by the inhibition of NF-kB signaling. suppression of Sirt1 enhances the NF-κB signaling resulting in inflammatory responses[54]. The most notable finding was that the Sirt1 were fully reduced by insulin resistance in vitro. Insulin resistance induced the reduction of Sirt1 production via activation of HIF1α/COX2. The disruption of Sirt1 was improved by ELT administration in MHE rats. We identified the reduction of Sirt1 through the reduction of ELT levels. In this study, we found that ELT is involved in regulating the Sirt1 production involved in synaptic formation in the brains of MHE rats.

Sirt1 gain-of-function is neuroprotective in models of neurodegeneration, which are relevant to Alzheimer's disease and amyotrophic lateral sclerosis (ALS), respectively [55]. In the adult brain, Sirt1 can also modulate synaptic plasticity and memory formation [56]. In addition to its importance during normal brain aging, Sirt1 has also been shown to ameliorate a number of neurodegenerative disorders including Alzheimer's disease [57], Parkinson's disease [58], Huntington's disease [59], motor neuron diseases [60] and multiple sclerosis [61]. Sirt1 knockout animals have morphologic alterations in neuronal structure, exhibiting dendrites with decreased complexity and shorter branches by Golgi staining [62]. Studies using electron microscopy to examine synaptic morphology show that inhibiting Sirt1 decreases synaptic inputs to hippocampal neurons [63]. Sirt1 knockout mice have impaired hippocampal-dependent memory that is associated with decreased long-term potentiation (LTP) in the CA1 region of the hippocampus [24−26]. Sirt1 is indispensable for normal synaptic plasticity and memory [24−26, 63]. We found that ELT is a critical factor for improving insulin resistance, and that decreased ELT is associated with insulin resistance in MHE brains. We revealed that ELT may act through inhibition of HIF1α and COX2, and upregulation of Sirt1 to induce synaptic formation and lead to cognitive enhancement. These findings indicate that ELT may enhance synaptic proteins under MHE conditions in which normal synapse is impaired via Sirt1.

Glial cell line-derived neurotrophic factor (GDNF) is a member of the transforming growth factor superfamily. It is a potent neurotrophic factor active on a broad spectrum of neuronal types and has neuroprotective effects in several experimental paradigms of neural injuries [64, 65]. GDNF has remarkable regenerative, restorative and neurotrophic effects upon nigrostriatal dopaminergic neurons [66]. GDNF exposure significantly regained cognitive abilities of atrophied neurons [67]. The perturbed production and activity of GDNF has been shown responsible for impaired neural regeneration observed in clinical tissues and experimental diabetic models [68], and depletion of GDNF seems to be linked the pathology, symptoms and cognitive deterioration of some neurological diseases such as Alzheimer's disease (AD) [69, 70]. In the present study, we obtained results showing that administration of ELT immediately facilitates memory function in MHE rats. Our finding that synaptic formation is facilitated by ELT provides compelling evidence that ELT may be critically involved in long-term memory. Our study showed that the addition of ELT induced a further increase in synaptic proteins in insulin resistant cells.

Conclusion

Taken together, our findings combined with findings that insulin resistance in vivo support that insulin resistance combined with the reduction of MPL expression might be the common mechanism for the

pathogenesis of MHE. The results support our hypothesis that insulin resistance leads to a disruption of HIF1α/COX2/Sirt1 signal transduction pathways in events underlying memory ability, which are reversed by ELT treatment. Our findings also showed that treatment with ELT mitigated insulin resistance, dendritic spine loss, synaptic dysfunction and memory impairment in MHE rats. These findings highlight ELT as a promising potential treatment for MHE.

List Of Abbreviations

AD: Alzheimer's disease; BCA: bicinchoninic acid; BSA: bovine serum albumin; ELT: eltrombopag; FBS: fetal bovine serum; GDNF: Glial cell line-derived neurotrophic factor; HE: hepatic encephalopathy; HFD: high-fat diet; HIF1α: Hypoxia-inducible factor-1α; HIF1β: Hypoxia-inducible factor-1; HOMA-IR: homeostasis model of insulin resistance; i.p.: intraperitoneal injection; KRP: Krebs−Ringer phosphate buffer; LTP: long-term potentiation; MAP2B: microtubule-associated protein 2B; MHE: Minimal hepatic encephalopathy; MPL: thrombopoietin receptor; PBS: phosphate buffer saline; PDGF: Platelet-derived growth factor; PHNs: Primary hippocampal neurons; qPCR: Quantitative Real-time PCR; RT-PCR: Reverse Transcription-Polymerase Chain Reaction; Sirt1: sirtuin-1; TAA: thioacetamide; TPO: Thrombopoietin; vGlut1: vesicular glutamate transporter 1; WFT: water-finding task; YM: Y-maze

Declarations

Ethics approval and consent to participate

The study was approved by the Ethics Committee of the First Affiliated Hospital of Wenzhou Medical University.

Consent for publication

Not applicable

Availability of supporting data

The data that support the findings of this study are available from the corresponding author upon reasonable request.

Competing interests

The authors have declared no conflict of interest.

Funding

References

1. Ehrenreich, H., et al., *A hematopoietic growth factor, thrombopoietin, has a proapoptotic role in the brain.* Proc Natl Acad Sci U S A, 2005. **102**(3): p. 862-7.

2. Yang, M., et al., *Identification of TPO receptors on central nervous system-a preliminary report.* Zhongguo Shi Yan Xue Ye Xue Za Zhi, 2004. **12**(4): p. 494-7.

3. Li, L., et al., *c-Mpl and TPO expression in the human central nervous system neurons inhibits neuronal apoptosis.* Aging (Albany NY), 2020. **12**(8): p. 7397-7410.

4. Wu, W., et al., *Thrombopoietin could protect cerebral tissue against ischemia-reperfusion injury by suppressing NF-κB and MMP-9 expression in rats.* Int J Med Sci, 2018. **15**(12): p. 1341-1348.

5. Dame, C., et al., *Thrombopoietin gene expression in the developing human central nervous system.* Brain Res Dev Brain Res, 2003. **143**(2): p. 217-23.

6. Columbyova, L., M. Loda, and D.T. Scadden, *Thrombopoietin receptor expression in human cancer cell lines and primary tissues.* Cancer Res, 1995. **55**(16): p. 3509-12.

7. Ivanova, A., et al., *Expression pattern of the thrombopoietin receptor (Mpl) in the murine central nervous system.* BMC Dev Biol, 2010. **10**: p. 77.

8. Li, B., et al., *Thrombopoietin and its alternatively spliced form are expressed in human amygdala and hippocampus.* Blood, 1996. **87**(12): p. 5382-4.

9. Bajaj, J.S., et al., *The effect of fatigue on driving skills in patients with hepatic encephalopathy.* Am J Gastroenterol, 2009. **104**(4): p. 898-905.

10. Sharma, P., et al., *Critical flicker frequency: diagnostic tool for minimal hepatic encephalopathy.* J Hepatol, 2007. **47**(1): p. 67-73.

11. Burness, C.B., G.M. Keating, and K.P. Garnock-Jones, *Eltrombopag: A Review in Paediatric Chronic Immune Thrombocytopenia.* Drugs, 2016. **76**(8): p. 869-78.

12. Cancello, R., et al., *Reduction of macrophage infiltration and chemoattractant gene expression changes in white adipose tissue of morbidly obese subjects after surgery-induced weight loss.* Diabetes, 2005. **54**(8): p. 2277-2286.

13. Halberg, N., et al., *Hypoxia-inducible factor 1alpha induces fibrosis and insulin resistance in white adipose tissue.* Molecular & Cellular Biology, 2009. **29**(16): p. 4467.

14. Krishnan, J., et al., *Dietary obesity-associated Hif1α activation in adipocytes restricts fatty acid oxidation and energy expenditure via suppression of the Sirt2-NAD+ system.* Genes & Development, 2012. **26**(3): p. 259-70.

15. Lee, K.Y., et al., *The Differential Role of Hif1β/Arnt and the Hypoxic Response in Adipose Function, Fibrosis, and Inflammation.* Cell Metabolism, 2011. **14**(4): p. 491-503.

16. Semenza, G.L., *HIF-1: mediator of physiological and pathophysiological responses to hypoxia.* Journal of Applied Physiology, 2000. **88**(4): p. 1474-1480.

17. Keith, B., R.S. Johnson, and M.C. Simon, *HIF1α and HIF2α: sibling rivalry in hypoxic tumour growth and progression.* Nature Reviews Cancer, 2011. **12**(1): p. 9.

18. Ding, S., et al., *Insulin Resistance Disrupts the Interaction Between AKT and the NMDA Receptor and the Inactivation of the CaMKIV/CREB Pathway in Minimal Hepatic Encephalopathy.* Toxicol Sci, 2018. **161**(1): p. 208.

19. Albrecht, J., et al., *Extracellular concentrations of taurine, glutamate, and aspartate in the cerebral cortex of rats at the asymptomatic stage of thioacetamide-induced hepatic failure: modulation by ketamine anesthesia.* Neurochem Res, 2000. **25**(11): p. 1497-502.

20. Yamada, M., et al., *Implanted cannula-mediated repetitive administration of Abeta25-35 into the mouse cerebral ventricle effectively impairs spatial working memory.* Behav. Brain Res., 2005. **164**(2): p. 139-46.

21. Kawasumi, M., et al., *Targeted introduction of V642I mutation in amyloid precursor protein gene causes functional abnormality resembling early stage of Alzheimer's disease in aged mice.* Eur. J. Neurosci., 2004. **19**(10): p. 2826-2838.

22. Takikawa, A., et al., *HIF-1α in Myeloid Cells Promotes Adipose Tissue Remodeling Toward Insulin Resistance.* Diabetes, 2016: p. db160012.

23. Sun, C., et al., *SIRT1 Improves Insulin Sensitivity under Insulin-Resistant Conditions by Repressing PTP1B.* Cell Metabolism, 2007. **6**(4): p. 307-319.

24. Satoh, A., et al., *SIRT1 promotes the central adaptive response to diet restriction through activation of the dorsomedial and lateral nuclei of the hypothalamus.* Journal of Neuroscience, 2010. **30**(30): p. 10220-10232.

25. Matarese, G., et al., *Hunger-promoting hypothalamic neurons modulate effector and regulatory T-cell responses.* Proceedings of the National Academy of Sciences, 2013. **110**(15): p. 6193-6198.

26. Chang, H.-C. and L. Guarente, *SIRT1 mediates central circadian control in the SCN by a mechanism that decays with aging.* Cell, 2013. **153**(7): p. 1448-1460.

27. Kaushansky, K., *Thrombopoietin and the hematopoietic stem cell.* Blood, 1998. **92**(1): p. 1-3.

28. Li, B. and W. Dai, *Thrombopoietin and neurotrophins share a common domain.* Blood, 1995. **86**(4): p. 1643-4.

29. Methia, N., et al., *Oligodeoxynucleotides antisense to the proto-oncogene c-mpl specifically inhibit in vitro megakaryocytopoiesis.* Blood, 1993. **82**(5): p. 1395-401.

30. Semenza, G.L., *Hypoxia-inducible factor 1 (HIF-1) pathway.* Sci STKE, 2007. **2007**(407): p. cm8.

31. Liu, X., et al., *Hypercapnia Exacerbates the Blood-Brain Barrier Disruption Via Promoting HIF-1a Nuclear Translocation in the Astrocytes of the Hippocampus: Implication in Further Cognitive Impairment in Hypoxemic Adult Rats.* Neurochem Res, 2020. **45**(7): p. 1674-1689.

32. Cao, Y., et al., *Isoflurane-induced postoperative cognitive dysfunction is mediated by hypoxia-inducible factor-1α-dependent neuroinflammation in aged rats.* Mol Med Rep, 2018. **17**(6): p. 7730-7736.

33. Cho, Y., et al., *Activating Injury-Responsive Genes with Hypoxia Enhances Axon Regeneration through Neuronal HIF-1α.* Neuron, 2015. **88**(4): p. 720-34.

34. Leiton, C.V., et al., *Astrocyte HIF-2α supports learning in a passive avoidance paradigm under hypoxic stress.* Hypoxia (Auckl), 2018. **6**: p. 35-56.

35. López, D.E. and S.J. Ballaz, *The Role of Brain Cyclooxygenase-2 (Cox-2) Beyond Neuroinflammation: Neuronal Homeostasis in Memory and Anxiety.* Mol Neurobiol, 2020. **57**(12): p. 5167-5176.

36. Zhao, J., et al., *Neuroinflammation induced by lipopolysaccharide causes cognitive impairment in mice.* Sci Rep, 2019. **9**(1): p. 5790.

37. Iqbal, S., et al., *Succinamide Derivatives Ameliorate Neuroinflammation and Oxidative Stress in Scopolamine-Induced Neurodegeneration.* Biomolecules, 2020. **10**(3).

38. Echeverria, V., et al., *Sorafenib inhibits nuclear factor kappa B, decreases inducible nitric oxide synthase and cyclooxygenase-2 expression, and restores working memory in APPswe mice.* Neuroscience, 2009. **162**(4): p. 1220-31.

39. Martins, J.O., et al., *Insulin suppresses LPS-induced iNOS and COX-2 expression and NF-kappaB activation in alveolar macrophages.* Cell Physiol Biochem, 2008. **22**(1-4): p. 279-86.

40. Rajasekar, N., et al., *Protection of streptozotocin induced insulin receptor dysfunction, neuroinflammation and amyloidogenesis in astrocytes by insulin.* Neuropharmacology, 2014. **86**: p. 337-52.

41. Lei, R., et al., *HIF-1α promotes the keloid development through the activation of TGF-β/Smad and TLR4/MyD88/NF-κB pathways.* Cell Cycle, 2019. **18**(23): p. 3239-3250.

42. Rius, J., et al., *NF-kappaB links innate immunity to the hypoxic response through transcriptional regulation of HIF-1alpha.* Nature, 2008. **453**(7196): p. 807-11.

43. Huang, M., et al., *Regulation of COX-2 expression and epithelial-to-mesenchymal transition by hypoxia-inducible factor-1α is associated with poor prognosis in hepatocellular carcinoma patients post TACE surgery.* Int J Oncol, 2016. **48**(5): p. 2144-54.

44. Jung, Y.J., et al., *IL-1beta-mediated up-regulation of HIF-1alpha via an NFkappaB/COX-2 pathway identifies HIF-1 as a critical link between inflammation and oncogenesis.* Faseb j, 2003. **17**(14): p. 2115-7.

45. Xuan, O., et al., *SIRT1 Positively Regulates Autophagy and Mitochondria Function in Embryonic Stem Cells Under Oxidative Stress.* Stem Cells, 2014. **32**(5): p. 1183–1194.

46. Szkudelski, T. and K. Szkudelska, *Anti-diabetic effects of resveratrol.* Annals of the New York Academy of Sciences, 2011. **1215**(1): p. 34–39.

47. Chao, J., et al., *Dietary oxyresveratrol prevents parkinsonian mimetic 6-hydroxydopamine neurotoxicity.* Free Radical Biology & Medicine, 2008. **45**(7): p. 1019-1026.

48. Pulla, V.K., et al., *Can targeting SIRT-1 to treat type 2 diabetes be a good strategy? A review.* Expert Opinion on Therapeutic Targets, 2012. **16**(16): p. 819-832.

49. Wang, R.H., et al., *Hepatic Sirt1 deficiency in mice impairs mTorc2/Akt signaling and results in hyperglycemia, oxidative damage, and insulin resistance.* Journal of Clinical Investigation, 2011. **121**(11): p. 4477-4490.

50. Yoshizaki, T., et al., *SIRT1 Exerts Anti-Inflammatory Effects and Improves Insulin Sensitivity in Adipocytes.* Molecular & Cellular Biology, 2009. **29**(5): p. 1363.

51. Milne, J.C. and J.M. Denu, *The Sirtuin family: therapeutic targets to treat diseases of aging.* Current Opinion in Chemical Biology, 2008. **12**(1): p. 11-17.

52. Milne, J.C., et al., *Small molecule activators of SIRT1 as therapeutics for the treatment of type 2 diabetes.* Nature, 2011. **450**(7170): p. 712-716.

53. Moynihan, K.A., et al., *Increased dosage of mammalian Sir2 in pancreatic beta cells enhances glucose-stimulated insulin secretion in mice.* Cell Metabolism, 2005. **2**(2): p. 105-117.

54. Franceschelli, S., et al., *A Novel Biological Role of α-Mangostin in Modulating Inflammatory Response Through the Activation of SIRT-1 Signaling Pathway.* J Cell Physiol, 2016. **231**(11): p. 2439-51.

55. Kim, D., et al., *SIRT1 deacetylase protects against neurodegeneration in models for Alzheimer's disease and amyotrophic lateral sclerosis.* Embo Journal, 2007. **26**(13): p. 3169-3179.

56. Gao, J., et al., *A novel pathway regulates memory and plasticity via SIRT1 and miR-134.* Nature, 2010. **466**(7310): p. 1105-1109.

57. Donmez, G., et al., *SIRT1 Suppresses β-Amyloid Production by Activating the α-Secretase Gene ADAM10.* Cell, 2010. **142**(2): p. 320-332.

58. Donmez, G., et al., *SIRT1 protects against α-synuclein aggregation by activating molecular chaperones.* Journal of Neuroscience the Official Journal of the Society for Neuroscience, 2012. **32**(1): p. 124-132.

59. Jeong, H., et al., *Sirt1 mediates neuroprotection from mutant huntingtin by activation of the TORC1 and CREB transcriptional pathway.* Nature Medicine, 2011. **18**(1): p. 159-165.

60. Han, S., et al., *Resveratrol upregulated heat shock proteins and extended the survival of G93A-SOD1 mice.* Brain Research, 2012. **1483**(45): p. 112–117.

61. Fonseca-Kelly, Z., et al., *Resveratrol neuroprotection in a chronic mouse model of multiple sclerosis.* Frontiers in Neurology, 2012. **3**: p. 84.

62. Michán, S., et al., *SIRT1 is essential for normal cognitive function and synaptic plasticity.* Journal of Neuroscience, 2010. **30**(29): p. 9695-9707.

63. Dietrich, M.O., et al., *Agrp neurons mediate Sirt1's action on the melanocortin system and energy balance: roles for Sirt1 in neuronal firing and synaptic plasticity.* Journal of Neuroscience, 2010. **30**(35): p. 11815-11825.

64. Lin, L.F., et al., *GDNF: a glial cell line-derived neurotrophic factor for midbrain dopaminergic neurons.* Science, 1993. **260**(5111): p. 1130-1132.

65. Lin, L.F., et al., *Purification and initial characterization of rat B49 glial cell line-derived neurotrophic factor.* Journal of Neurochemistry, 1994. **63**(2): p. 758–768.

66. Lang, A.E., et al., *Randomized controlled trial of intraputamenal glial cell line-derived neurotrophic factor infusion in Parkinson disease.* Annals of Neurology, 2003. **9**(5): p. 589-595.

67. Pertusa, M., et al., *Expression of GDNF transgene in astrocytes improves cognitive deficits in aged rats.* Neurobiology of Aging, 2008. **29**(9): p. 1366-1379.

68. Du, F., et al., *Loss of enteric neurons accompanied by decreased expression of GDNF and PI3K/Akt pathway in diabetic rats.* Neurogastroenterology & Motility the Official Journal of the European Gastrointestinal Motility Society, 2009. **21**(11): p. 1229–e114.

69. Pyo, H., et al., *Mitogen-activated protein kinases activated by lipopolysaccharide and beta-amyloid in cultured rat microglia.* Neuroreport, 1998. **9**(5): p. 871-874.

70. Savage, M.J., et al., *Activation of c-Jun N-terminal kinase and p38 in an Alzheimer's disease model is associated with amyloid deposition.* Journal of Neuroscience the Official Journal of the Society for Neuroscience, 2002. **22**(9): p. 3376.

Tables

Table 1: The effects of ELT administration on insulin resistance in MHE groups of rats			
Groups	Fasting plasma glucose (mg/dl)	Plasma insulin (ng/ml)	HOMA-IR
Control	108.3±20.57	1.8±0.31	8.1±1.01
MHE	170.7±22.68**	4.3±0.97**	39.6±3.71**
MHE+5ELT	167.7±19.91	4.1±0.82	38.4±2.27
MHE+25ELT	111.6±12.34##	1.9±0.28##	8.3±1.49##

*P<0.05, **P<0.01 vs Con group. #P <0.05, ##P <0.01 vs MHE group.

Figures

Figure 1

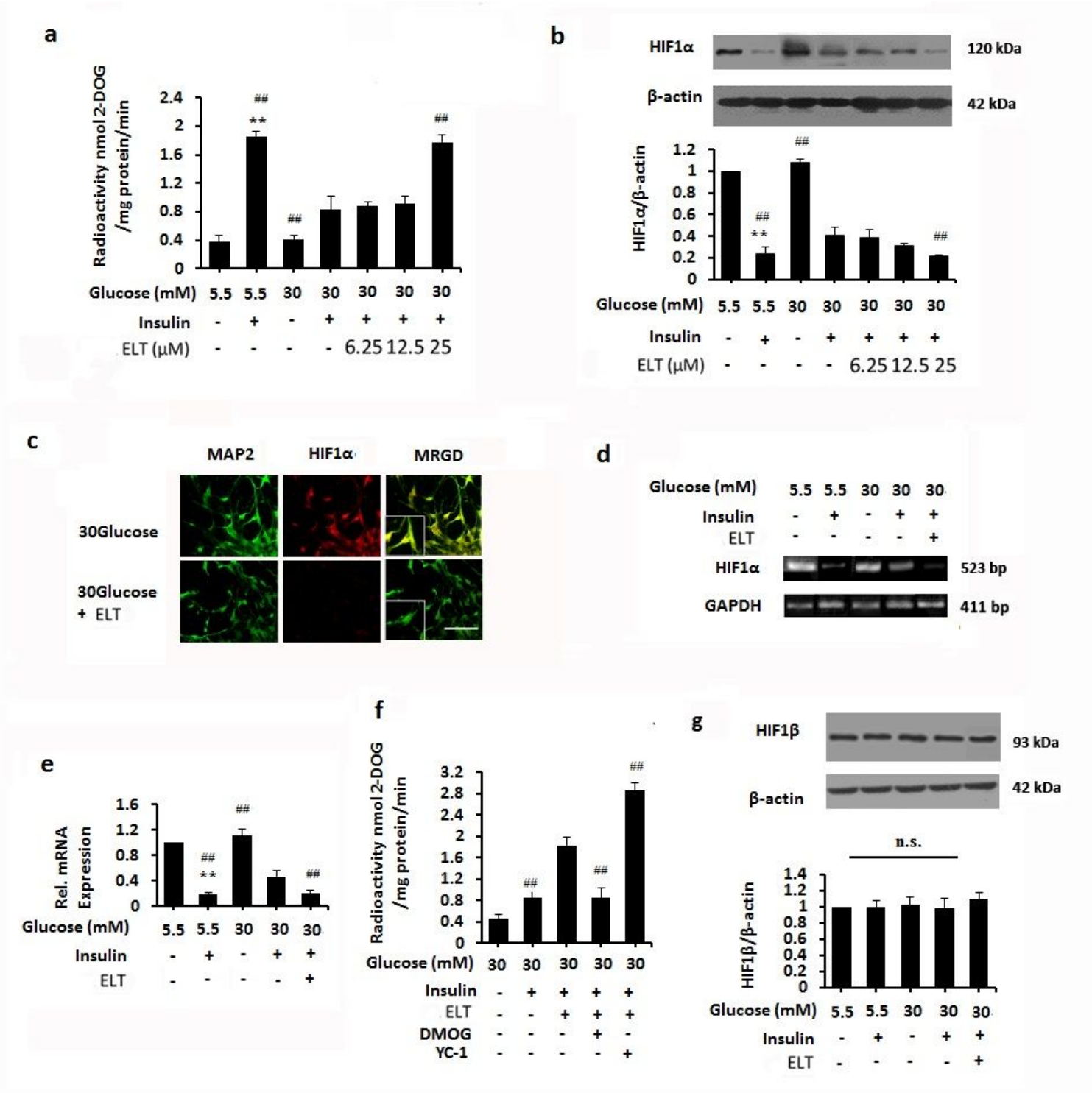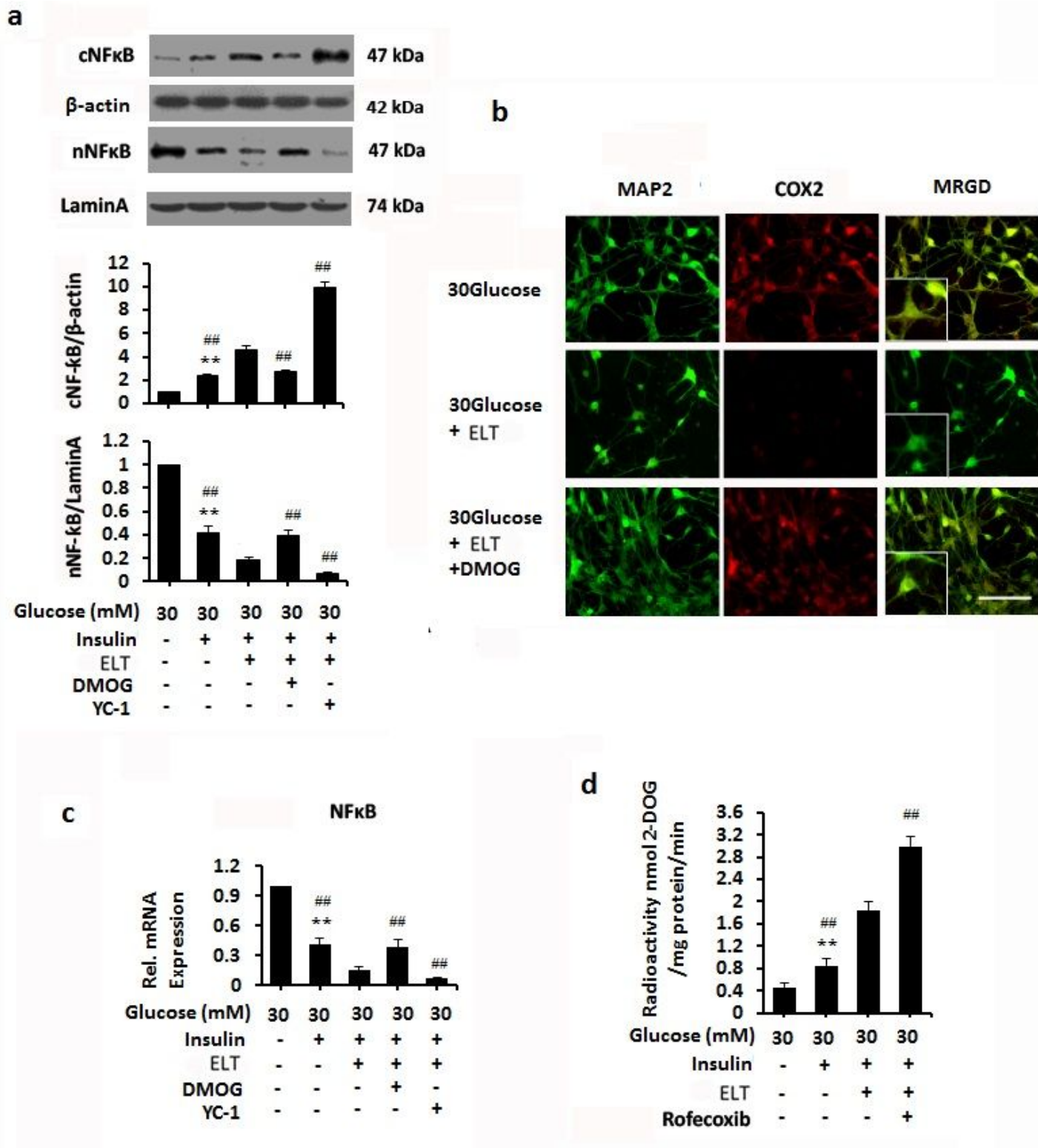ELT reduced Insulin -mediated HIF1α in insulin resistant PHNs (a) Measurement of 2-NBDG uptake for PHNs treated with or without various concentration of ELT (6.25, 12.5 and 25 μM) after preincubation of 5.5 mM or 30mM glucose in the absence or presence of 100 nM insulin. Data are shown as mean± SD. *P <0.05, **P <0.01 vs 5.5 mM glucose -treated group. #P <0.05, ##P <0.01 vs 30mM glucose+100nM insulin

-treated group. (b) IB analysis of lysate from PHNs treated with 5.5 mM or 30mM glucose after preincubation of various concentration of ELT (6.25, 12.5 and 25 μM) in the absence or presence of 100 nM insulin using anti-HIF1α and anti-β-actin antibodies and subsequent densitometry. (c) Double immunofluorescence staining of PHNs treated with 30mM glucose after preincubation with ELT (25 μM) in the absence or presence of 100 nM insulin using antibodies against HIF1α (Red), MAP2 (Green). (d, e) RT-PCR (d) or Q-PCR (e) analysis of HIF1α mRNAs of PHNs treated with 5.5 mM or 30mM glucose after preincubation of 25 μM ELT in the absence or presence of 100 nM insulin. (f) Measurement of 2-NBDG uptake for PHNs treated with DMOG or YC-1 after preincubation of 25 μM ELT in the presence of 5.5 mM or 30mM glucose together with 100 nM insulin. (g) IB analysis of lysate from PHNs treated with 5.5 mM or 30 mM glucose after preincubation of ELT (25 μM) in the absence or presence of 100 nM insulin using anti-HIF1β and anti-β-actin antibodies and subsequent densitometry. Data are shown as mean± SD. *P <0.05, **P <0.01 vs 5.5 mM glucose -treated group. #P <0.05, ##P <0.01 vs 30mM glucose+100nM insulin -treated group. n.s., not significant. Scale bar, 25 μm.

Figure 2

ELT decreased inflammation via HIF1α in insulin resistant PHNs (a) IB analysis of nuclear fraction and cytoplasmic fraction of PHNs treated with DMOG or YC-1 after preincubation with 25 μM ELT in the presence of 30mM glucose together with 100 nM insulin using anti-NF-◻B and anti-β-actin antibodies and subsequent densitometry. (b) Double immunofluorescence staining of PHNs treated with DMOG after preincubation with 25 μM ELT in the presence of 30mM glucose together with 100 nM insulin using

antibodies against COX2 (red), MAP2 (green). (c) RT-PCR analysis of NF-𝜅B mRNAs of PHNs treated with DMOG or YC-1 after preincubation with 25 μM ELT in the presence of 30mM glucose. (d) Measurement of 2-NBDG uptake for PHNs treated with Rofecoxib after preincubation with 25 μM ELT in the presence of 30mM glucose together with or without 100 nM insulin. Data are shown as mean± SD. *P <0.05, **P <0.01 vs 30mM glucose-treated group. #P <0.05, ##P <0.01 vs 30mM glucose+ELT+100nM insulin -treated group. Scale bar, 25 μm.
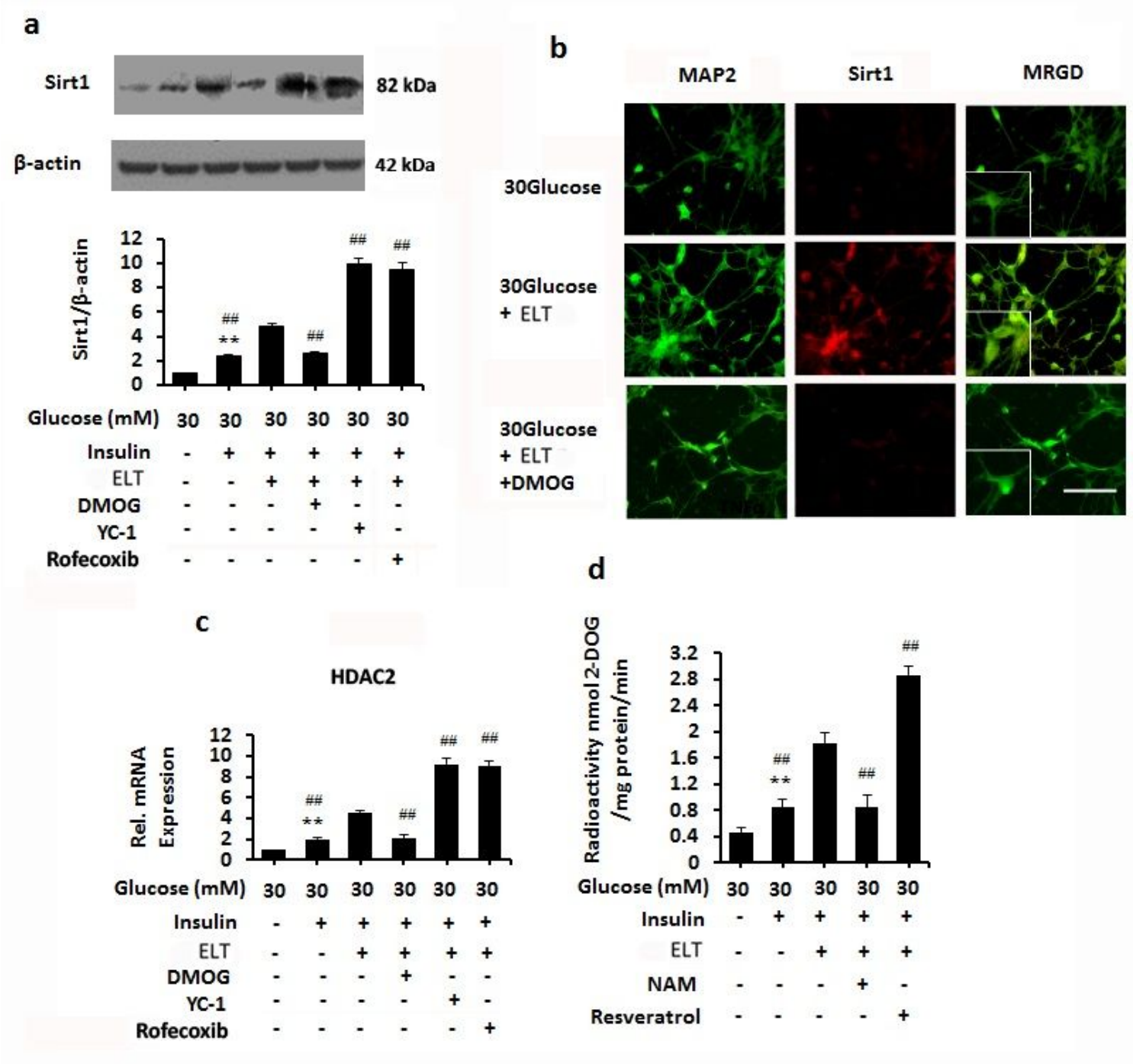
Figure 3

ELT increased insulin-mediated Sirt1 expression via HIF1α/ COX2 in insulin resistant PHNs (a) IB analysis of PHNs treated with DMOG/YC-1/Rofecoxib after preincubation with 25 μM ELT in the presence of

30mM glucose together with or without 100 nM insulin using antibodies against Sirt1 and anti-β-actin and subsequent densitometry. (b) Double immunofluorescence staining of PHNs treated with DMOG after preincubation with 25 μM ELT in the presence of 30mM glucose together with 100 nM insulin using antibodies against Sirt1(Red), MAP2 (Green). (c) RT-PCR analysis of HDAC2 mRNAs of PHNs treated with DMOG/YC-1/Rofecoxib after preincubation with 25 μM ELT in the presence of 30mM glucose. (d) Measurement of 2-NBDG uptake for PHNs treated with NAM or resveratrol after preincubation of 25 μM ELT in the presence of 30mM glucose together with or without 100 nM insulin. Data are shown as mean± SD. *P <0.05, **P <0.01 vs 30mM glucose-treated group. #P <0.05, ##P <0.01 vs 30mM glucose+ELT+100nM insulin -treated group. Scale bar, 25 μm.
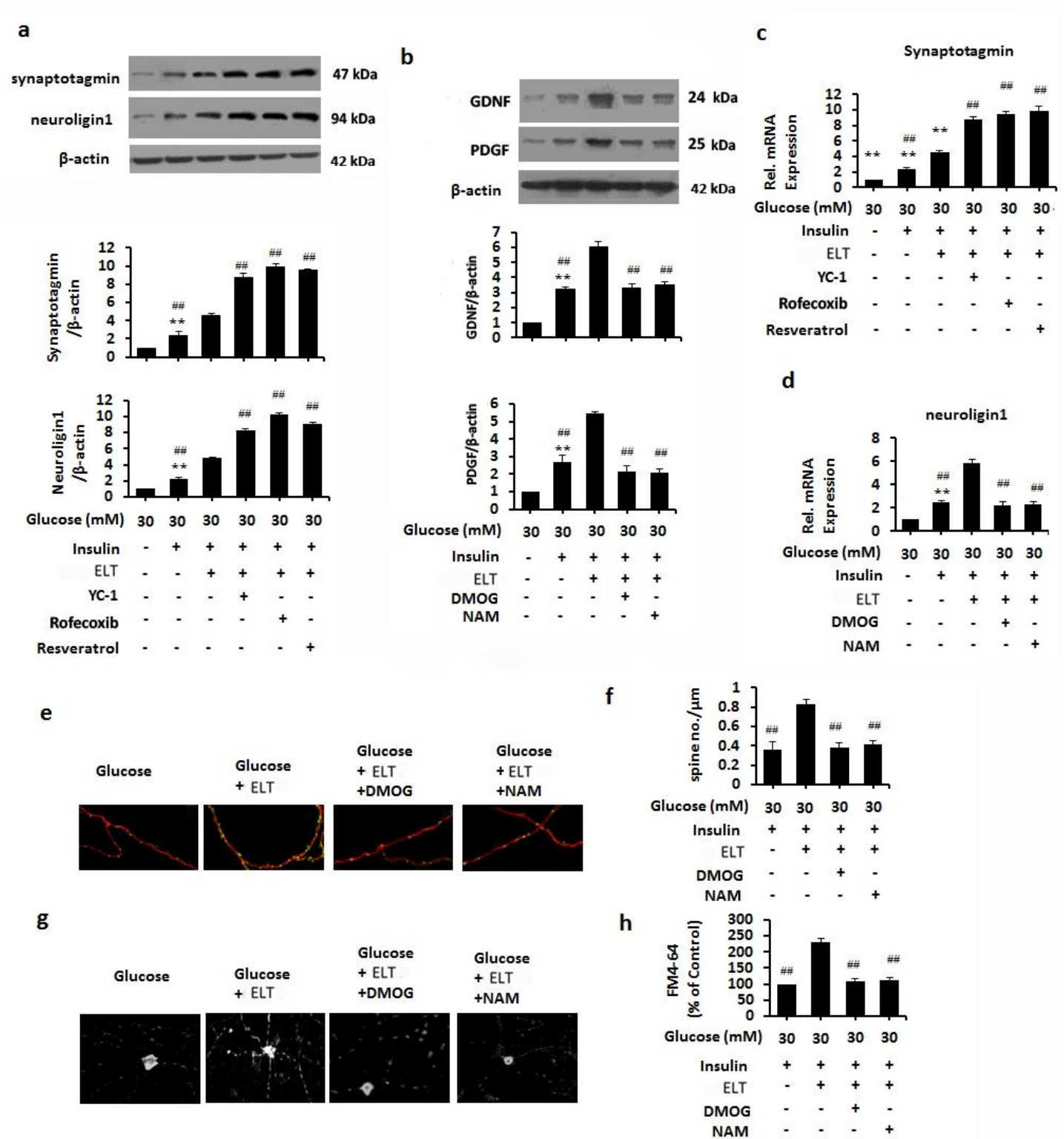
a

synaptotagmin — 47 kDa

neuroligin1 — 94 kDa

β-actin — 42 kDa

Glucose (mM)	30	30	30	30	30	30
Insulin	-	+	+	+	+	+
ELT	-	-	+	+	+	+
YC-1	-	-	-	+	-	-
Rofecoxib	-	-	-	-	+	-
Resveratrol	-	-	-	-	-	+

Synaptotagmin /β-actin

Neuroligin1 /β-actin

b

GDNF — 24 kDa

PDGF — 25 kDa

β-actin — 42 kDa

GDNF/β-actin

PDGF/β-actin

Glucose (mM)	30	30	30	30	30
Insulin	-	+	+	+	+
ELT	-	-	+	+	+
DMOG	-	-	-	+	-
NAM	-	-	-	-	+

c

Synaptotagmin

Rel. mRNA Expression

Glucose (mM)	30	30	30	30	30	30
Insulin	-	+	+	+	+	+
ELT	-	-	+	+	+	+
YC-1	-	-	-	+	-	-
Rofecoxib	-	-	-	-	+	-
Resveratrol	-	-	-	-	-	+

d

neuroligin1

Rel. mRNA Expression

Glucose (mM)	30	30	30	30	30
Insulin	-	+	+	+	+
ELT	-	-	+	+	+
DMOG	-	-	-	+	-
NAM	-	-	-	-	+

e

Glucose | Glucose + ELT | Glucose + ELT +DMOG | Glucose + ELT +NAM

f

spine no./μm

Glucose (mM)	30	30	30	30
Insulin	+	+	+	+
ELT	-	+	+	+
DMOG	-	-	+	-
NAM	-	-	-	+

g

Glucose | Glucose + ELT | Glucose + ELT +DMOG | Glucose + ELT +NAM

h

FM4-64 (% of Control)

Glucose (mM)	30	30	30	30
Insulin	+	+	+	+
ELT	-	+	+	+
DMOG	-	-	+	-
NAM	-	-	-	+

Figure 4

ELT increased insulin-mediated synaptic formation via HIF1α/COX2/Sirt1 in insulin resistant PHNs. (a) IB analysis of PHNs treated with YC-1/Rofecoxib/ resveratrol preincubation of 25 μM ELT in the presence of 30mM glucose together with or without 100 nM insulin using antibodies against synaptotagmin/neuroligin1 and anti-β-actin and subsequent densitometry. (b) IB analysis of PHNs treated with DMOG/NAM after preincubation with 25 μM ELT in the presence of 30mM glucose together

with or without 100 nM insulin using antibodies against GDNF/PDGF and anti-β-actin and subsequent densitometry. (c) qPCR analysis of synaptotagmin mRNAs of PHNs treated with YC-1/Rofecoxib/resveratrol preincubation with 25 μM ELT in the presence of 30mM glucose together with or without 100 nM insulin. (d) qPCR analysis of neuroligin1 mRNAs of PHNs treated with DMOG/NAM after preincubation with 25 μM ELT in the presence of 30mM glucose together with or without 100 nM insulin. (e) Immunostaining of PHNs treated with DMOG/NAM preincubation of 25 μM ELT in the presence of 30mM glucose together with or without 100 nM insulin against MAP2B (red) and vGluT1 (green). Red signals indicate MAP2B for microtubule staining and green signals indicate vGluT1 for detecting excitatory synapses. (f) Synaptic density was analyzed by counting green signals (vGluT1-positive dendriticspines) using ImageJ, and expressed per 1 μm of apical dendrite. (g) Representative image of FM4-64 staining of functional presynaptic terminals in PHNs treated with DMOG/NAM after preincubation of 25 μM ELT in the presence of 30mM glucose together with or without 100 nM insulin. The (h) panel indicates quantitative analysis of changes showed on average in FM4-64puncta intensity. Data are shown as mean± SD. *P<0.05, **P<0.01 vs 30mM glucose-treated group. #P <0.05, ##P <0.01 vs 30mM glucose+ELT+100nM insulin -treated group. Scale bar, 25 μm.
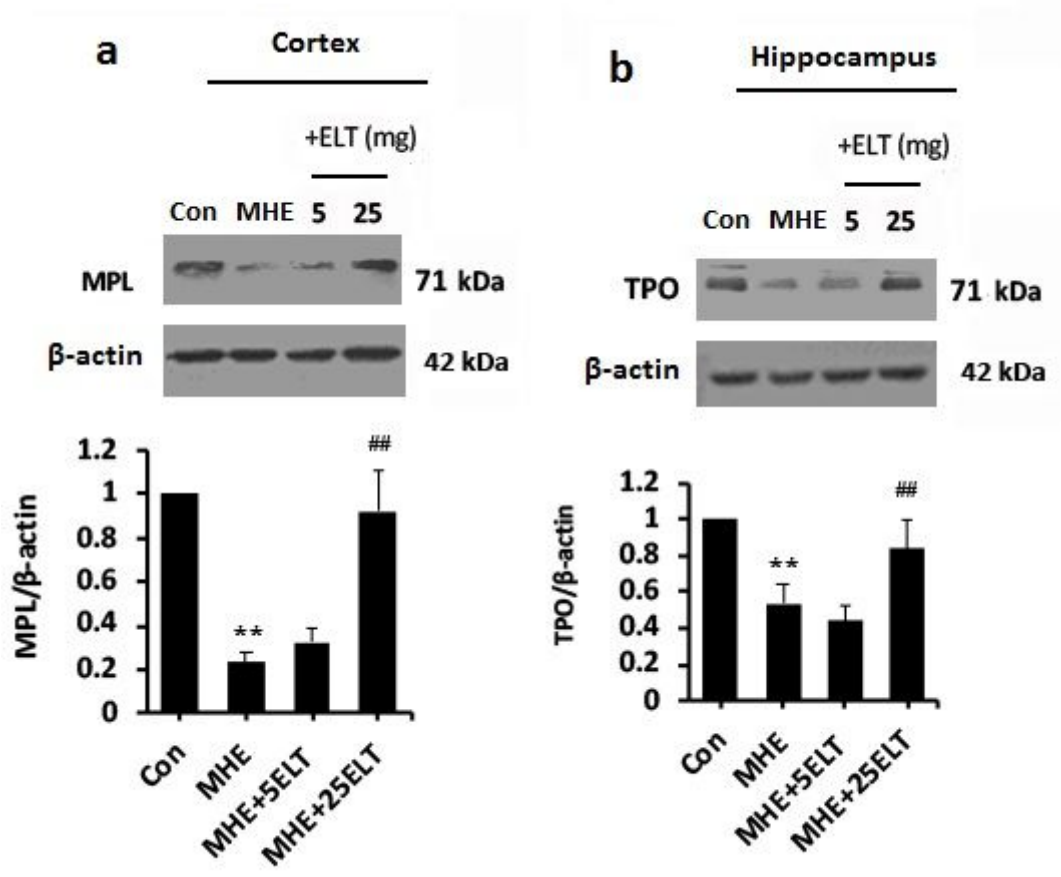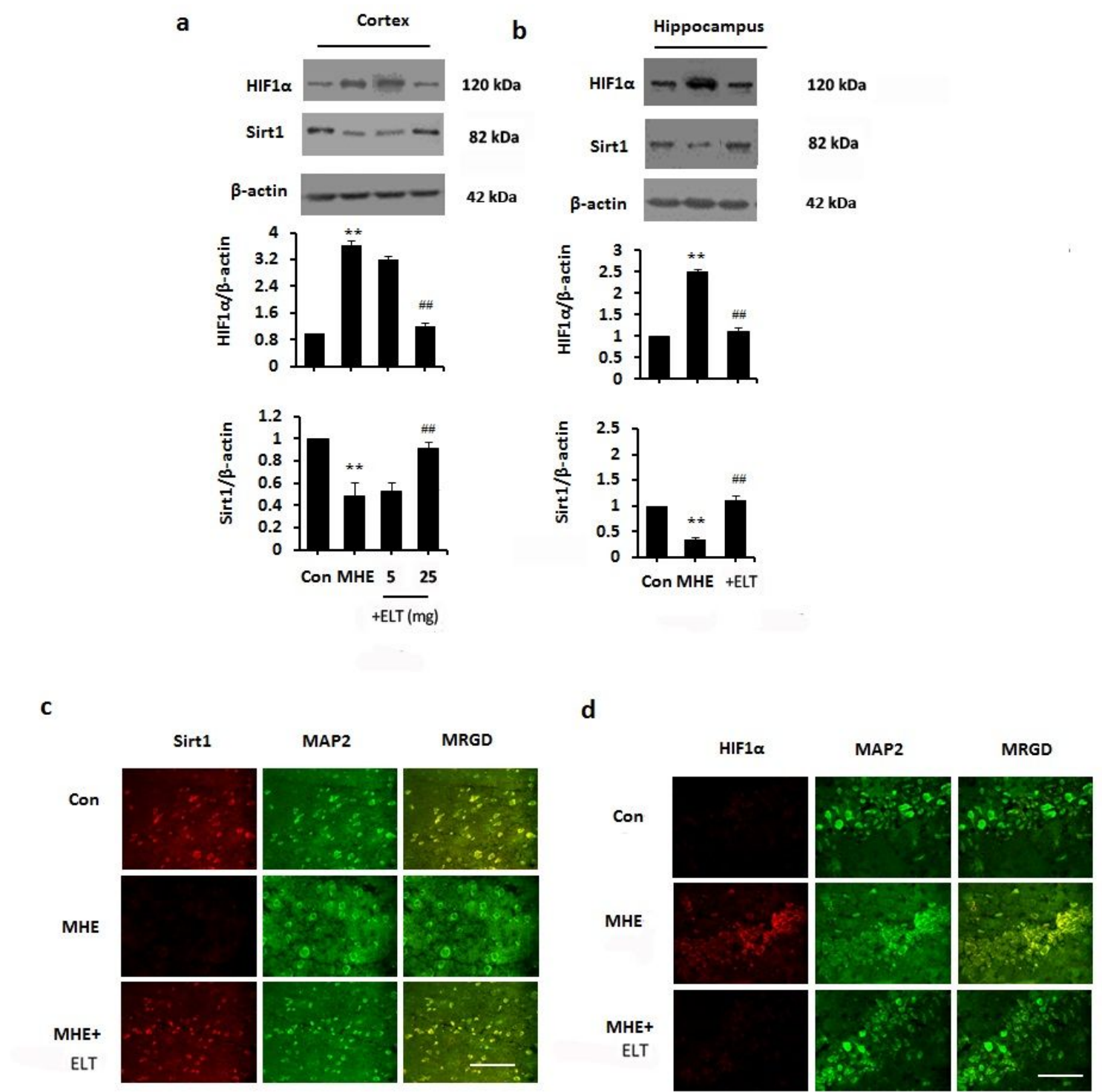

Figure 5

ELT increased MPL expression in MHE rats (a) IB analysis of cortical lysates from MHE rats administered with two dose (5, 25mg) of ELT using antibodies against MPL and β-actin and subsequent densitometry.
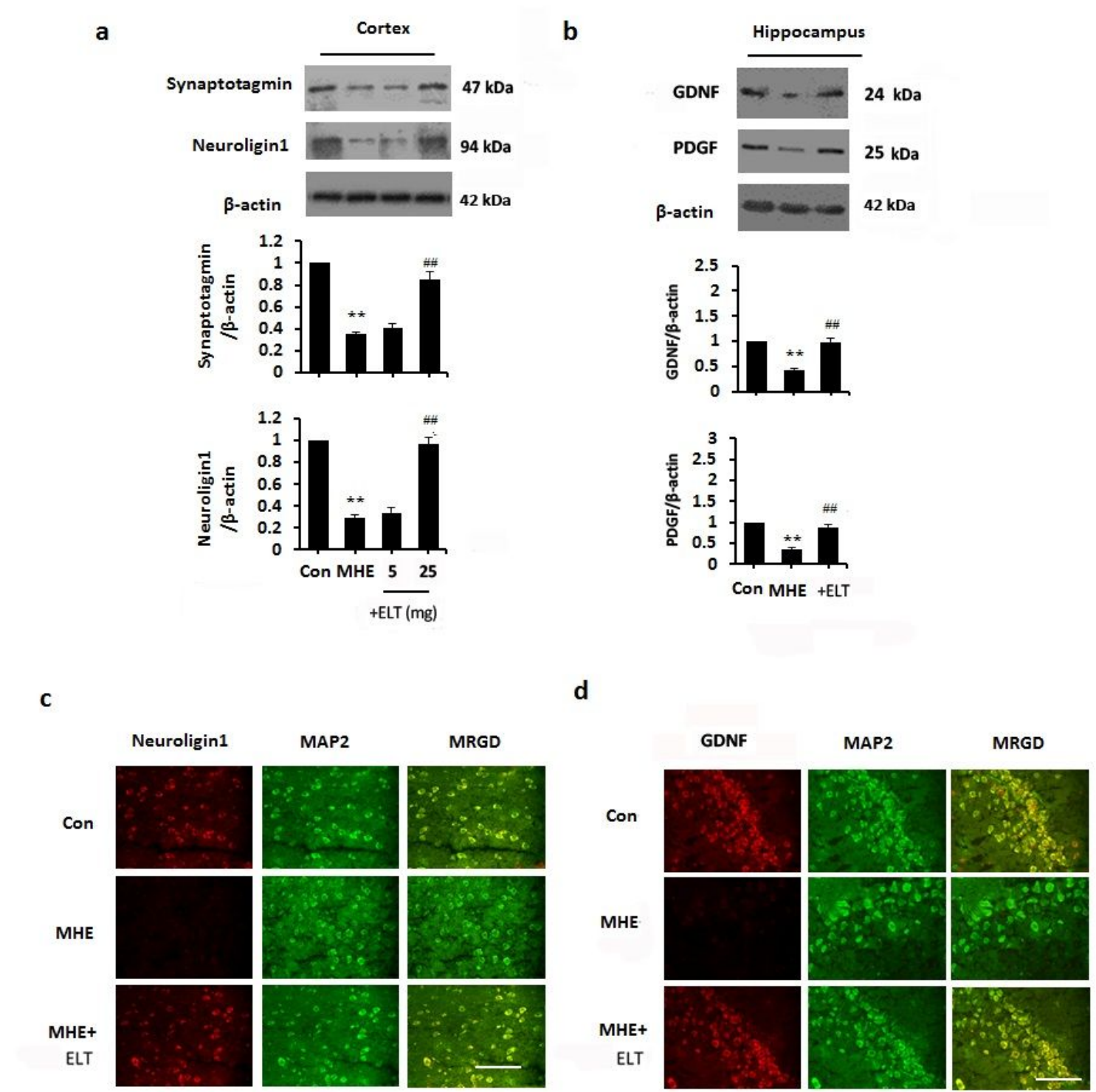
(b) IB analysis of hippocampal lysates from MHE rats administered with two dose (5, 25mg) of ELT using antibodies against TPO and β-actin and subsequent densitometry. Data are shown as mean± SD. *P <0.05, **P <0.01 vs Con group. #P <0.05, ##P <0.01 vs MHE model group. Scale bar, 25 μm. MRGD, merged image. Con, control.

Figure 6

ELT improved HIF1α/Sirt1 signaling pathway in MHE rats (a) IB analysis of cortical homogenates from MHE rats administered with various concentrations of ELT (5, 25mg) using antibodies against

HIF1α/Sirt1 and β-actin and subsequent densitometry. (b) IB analysis of hippocampal homogenates from MHE rats after administration with 25mg ELT using antibodies against HIF1α/Sirt1 and β-actin and subsequent densitometry. (c) Immunostaining of free-floating cortical sections from MHE rats after administration with 25mg ELT using antibodies against Sirt1 (red) and MAP2 (green). (d) Immunostaining of free-floating hippocampal sections from MHE rats after administration with 25mg ELT using antibodies against HIF1α (red) and MAP2 (green). Data are shown as mean± SD. *P <0.05, **P <0.01 vs Con group. #P <0.05, ##P <0.01 vs MHE model group. Scale bar, 25 μm. MRGD, merged image. Con, control.

Figure 7

ELT improved destruction of synaptogenesis in MHE rats (a) IB analysis of cortical homogenates from MHE rats administered with various concentrations of ELT (5, 25mg) using antibodies against synaptotagmin/ neuroligin1 and β-actin and subsequent densitometry. (b) IB analysis of hippocampal homogenates from MHE rats after administration with 25mg ELT using antibodies against GDNF/PDGF and β-actin and subsequent densitometry. (c) Immunostaining of free-floating cortical sections from MHE rats after administration with 25mg ELT using antibodies against neuroligin (red) and MAP2 (green). (d) Immunostaining of free-floating hippocampal sections from MHE rats after administration with 25mg ELT using antibodies against GDNF (red) and MAP2 (green). Scale bar, 25 μm. Data are shown as mean± SD. *P <0.05, **P <0.01 vs Con group. #P <0.05, ##P <0.01 vs MHE model group. Scale bar, 25 μm. MRGD, merged image. Con, control.

Supplementary Files

This is a list of supplementary files associated with this preprint. Click to download.

- FigureS1.tif
- FigureS2.tif